Variable Reduction Sequences for Axial (L) and Chelate Ligands (N∧N) in Rhenium(I) Complexes $[(N\wedge N)Re(CO)_3(L)]^n$

Sascha Berger, Axel Klein, and Wolfgang Kaim*

Institut für Anorganische Chemie, Universität Stuttgart, Pfaffenwaldring 55, D-70550 Stuttgart, Germany

Jan Fiedler

J. Heyrovsky Institute of Physical Chemistry, Academy of Sciences of the Czech Republic,
Dolejškova 3, CZ-18223 Prague, Czech Republic

Received March 12, 1998

The rhenium(I) compounds $[(N\wedge N)Re(CO)_3(MQ)](PF_6)_2$ (N∧N = 2,2′-bipyridine (bpy), 2,2′-bipyrimidine (bpym), 3,3′-bipyridazine (bpdz), or 1,4,7,10-tetraazaphenanthrene (tap) and MQ^+ = *N*-methyl-4,4′-bipyridinium) undergo four one-electron reduction steps which could be analyzed using cyclic voltammetry, EPR, IR, and UV/vis spectroelectrochemistry. Due to the rather low-lying π^* orbital of tap, the corresponding compound shows electron uptake by N∧N each time before MQ^+ is reduced. The opposite is observed for the complexes of the other chelate ligands N∧N, however, and the $\pi^*(N\wedge N)$ orbital aproaches the $\pi^*(MQ^+)$ level in the order bpy < bpym < bpdz. Remarkably, the reduction processes of MQ^+ and bpdz in $[(bpdz)Re(CO)_3(MQ)](PF_6)_2$ are separated by only 74 mV as deduced from IR spectroelectrochemical analysis. On reduction of the related compound $[(bpy)Re(CO)_3(mpz)](PF_6)_2$ (mpz^+ = *N*-methylpyrazinium), the first two electrons are added to the axial ligand which has a lower-lying π^* orbital than MQ^+ and cannot undergo intramolecular twisting.

Introduction

Coordination compounds are well suited to study intramolecular electron-transfer[1] phenomena because their components (ligands and metal centers) usually exist in well-defined structures and orientations, as implied by the term “coordination”. Furthermore, metal centers can participate in electron transfer, or at least become involved in the activation of the ligands. The *fac*-tricarbonylrhenium(I) complexes $[(N\wedge N)Re(CO)_3(MQ)]^{2+}$ (MQ^+ = *N*-methyl-4,4′-bipyridinium, N∧N = α-diimine) were thus previously used to study photoinduced intramolecular electron transfer:[2] irradiation of these “intramolecular chromophore−quencher” complexes[2] was shown to produce an N∧N-centered MLCT excited state $^*[(N\wedge N^{\bullet-})Re^{II}(CO)_3(MQ^+)]^{2+}$ which then converted to the more stable MQ-based MLCT state $^*[(N\wedge N)Re^{II}(CO)_3(MQ^\bullet)]^{2+}$ in an intramolecular oxidative quenching process leading to charge separation. It was then shown that these complexes can be reduced in up to four one-electron steps;[2] however, the localization of the added electron(s) and thus the direct determination of the electronic structures of the thus generated species remained open for further investigation.

In this paper we describe five compounds $[(N\wedge N)Re(CO)_3(L)]^{2+}$ to address the following questions:

(i) What techniques are best suited to define the locations of added electrons in the redox series $[(N\wedge N)Re(CO)_3(L)]^n$ (n = 2+, +, 0, −)?

(ii) Is it possible to change the sequence of added electrons by modifying the chelate ligand N∧N or the axial ligand L^+?

Question (i) was approached using EPR spectroscopy for the first reduced and therefore paramagnetic state; in addition, all spectroelectrochemically accessible states were studied by UV/vis absorption spectroscopy and by IR spectroscopy in the carbonyl stretching region. CO vibrational spectroscopy is well suited for monitoring changes in multielectron redox series,[3,4] and UV/vis spectroelectrochemistry can be applied considering the available data on reduced α-diimine, 4,4′-bipyridinium, and *N*-methylpyrazinium π systems.[5−7] The spectroscopic data will finally be correlated with the observed shifts of electrochemical potentials.

Since both the chelating α-diimine and the monodentate L^+ ligand can undergo two reversible reduction processes[5−7] before

---

[1] Isied, S. S., Ed. *Electron-Transfer Reactions*; Advances in Chemistry Series 253; American Chemical Society: Washington, DC, 1997.

[2] (a) Westmoreland, T. D.; Le Bozec, H.; Murray, R. W.; Meyer, T. J. *J. Am. Chem. Soc.* **1983**, *105*, 5952. (b) Chen, P.; Danielson, E.; Meyer, T. J. *J. Phys. Chem.* **1988**, *92*, 3708. (c) Chen, P.; Curry, M.; Meyer, T. J. *Inorg. Chem.* **1989**, *28*, 2271. (d) Schoonover, J. R.; Chen, P.; Bates, W. D.; Dyer, R. B.; Meyer, T. J. *Inorg. Chem.* **1994**, *33*, 793.

[3] (a) Geiger, W. E.; Van Order, N., Jr.; Pierce, D. T.; Bitterworf, T. E.; Rheingold, A. L.; Chasteen, N. D. *Organometallics* **1991**, *10*, 2403. (b) Atwood, C. G.; Geiger, W. E. *J. Am. Chem. Soc.* **1993**, *115*, 5310. (c) Zhang, Y.; Gosser, D. K.; Rieger, P. H.; Sweigart, D. A. *J. Am. Chem. Soc.* **1991**, *113*, 4062.

[4] (a) Kaim, W.; Bruns, W.; Kohlmann, S.; Krejcik, M. *Inorg. Chim. Acta* **1995**, *229*, 143. (b) Bruns, W.; Kaim, W.; Waldhör, E.; Krejcik, M. *Inorg. Chem.* **1995**, *34*, 663.

[5] (a) Braterman, P. S.; Song, J.-I. *J. Org. Chem.* **1991**, *56*, 4678. (b) Braterman, P. S.; Song, J.-I.; Wimmer, F. M.; Wimmer, S.; Kaim, W.; Klein, A.; Peacock, R. D. *Inorg. Chem.* **1992**, *31*, 5084. (c) Krejcik, M.; Zalis, S.; Ladwig, M.; Matheis, W.; Kaim, W. *J. Chem. Soc., Perkin Trans. 2* **1992**, 2007.

[6] (a) Deuchert, K.; Hünig, S. *Angew. Chem.* **1978**, *90*, 927; *Angew. Chem., Int. Ed. Engl.* **1978**, *17*, 875. (b) Hünig, S.; Berneth, H. *Top. Curr. Chem.* **1980**, *92*, 1. (c) Kaim, W.; Matheis, W. *Chem. Ber.* **1990**, *123*, 1323.

[7] (a) Waldhör, E.; Kaim, W.; Olabe, J. A.; Slep, L. D.; Fiedler, J. *Inorg. Chem.* **1997**, *36*, 2969. (b) For a related chromophore, see: Hilgers, F.; Kaim, W.; Schulz, A.; Zalis, S. *J. Chem. Soc., Perkin Trans. 2* **1994**, 135.

10.1021/ic980268f CCC: $15.00

Chart 1

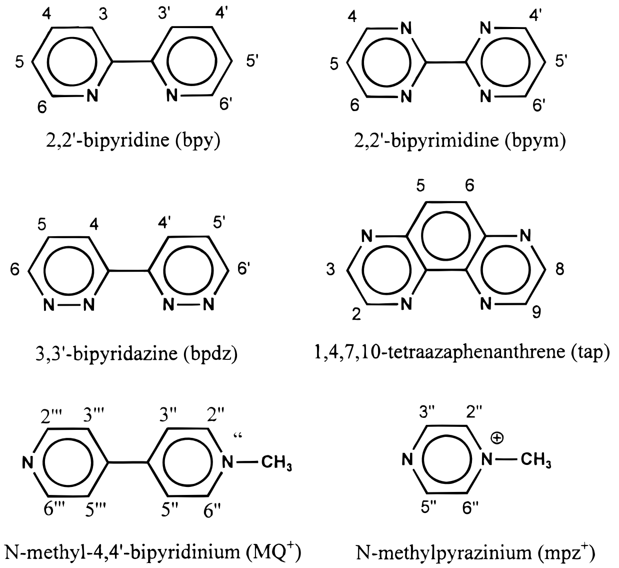

tricarbonylrhenium(I) is converted to a true Re^0 form, we expect up to four reversible waves to occur in the cyclovoltammograms of $[(N\wedge N)Re(CO)_3(L)](PF_6)_2$. As sufficiently different chelate ligands $N\wedge N$ in combination with $L^+ = MQ^+$, we chose the prototypical 2,2′-bipyridine (bpy)[8] as a moderate π acceptor and 2,2′-bipyrimidine (bpym),[9] 3,3′-bipyridazine (bpdz)[9a,10] and finally 1,4,7,10-tetraazaphenanthrene (tap)[11,12] as increasingly better π acceptors.[11b] Tap has been used as chelate ligand for a number of years[11,12] and was characterized as a ligand system in the ground and monoreduced state;[11] like bpdz,[9a] it has both a lower-lying π^* orbital than bpy and a higher MO coefficient of that LUMO at the coordinating nitrogen centers. It was shown that tap has the $b_1(\psi)$ as lowest unoccupied π MO (like bpy) although the $a_2(\chi)$ MO is situated rather close[11] (see Chart 1).

In yet a different approach, we substituted the axial ligand $L = MQ^+$ with the related *N*-methylpyrazinium (mpz^+) cation[7] in $[(bpy)Re(CO)_3(L)](PF_6)_2$. The mpz^+ cation is a good π acceptor ligand;[7a,13] unlike MQ^+,[2c,d,9b] however, it cannot change its electronic structure by intramolecular twisting.

Experimental Section

Instrumentation. EPR spectra were recorded in the X band on a Bruker System ESP 300 equipped with a Bruker ER035M gaussmeter and a HP 5350B microwave counter. ^{1}H NMR spectra were recorded on a Bruker AC 250 spectrometer, infrared spectra were obtained using a Philips PU 9800 FTIR instrument. UV/vis/NIR absorption spectra were recorded on a Bruins Instruments Omega 10 spectrophotometer. Cyclic voltammetry was carried out in acetonitrile/0.1 M Bu_4NPF_6 using a three-electrode configuration (1 mm glassy carbon electrode, Pt counter electrode, Ag/AgCl reference) and a PAR 273 potentiostat and function generator. The ferrocene/ferrocenium couple served as internal reference, and typical concentrations were 1 mM. Spectroelectrochemical measurements were performed using an optically transparent thin-layer electrode (OTTLE) cell[14] for IR and UV/vis spectra and a two-electrode capillary for EPR studies.[15]

Synthesis. The complexes $[(N\wedge N)Re(CO)_3(MQ)](PF_6)_2$ ($N\wedge N$ = bpy, bpym) were prepared according to literature procedures.[2,9b] The bpdz and tap analogues and compound $[(bpy)Re(CO)_3(mpz)](PF_6)_2$ were best obtained by first reacting the corresponding halide compound $(N\wedge N)Re(CO)_3Cl$[16,17] with equimolar amounts of $AgPF_6$ in CH_2Cl_2/CH_3OH (10/1, v/v), filtration of AgCl, and treatment of the resulting solution with $(MQ)(PF_6)$ or $(mpz)(PF_6)$.[2,13] The orange precipitates formed were washed with dichloromethane and dried under vacuum to yield about 30% of the products. Analysis (C, H, N) and ^{1}H NMR spectroscopy revealed varying amounts of CH_2Cl_2 as solvent of crystallization ($\delta = 5.32$ ppm). ^{1}H NMR (250 MHz, Me_2CO-d_6, 300 K) of $[(bpdz)Re(CO)_3(MQ)](PF_6)_2$: δ 4.64 (s, 3H, Me), 8.04 (m, 2H, $H^{3''',5'''}$), 8.45 (dd, 2H, $H^{5,5'}$), 8.51 (d, 2H, $H^{3'',5''}$), 8.83 (m, 2H, $H^{2''',6'''}$), 9.08 (dd, 2H, $H^{6,6'}$), 9.20 (d, 2H, $H^{2'',6''}$), 9.68 (dd, 2H, $H^{4,4'}$); $J(H^{2'',3'';5'',6''}) = 6.8$ Hz, $J(H^{2''',3'''}) = 5.2$ Hz, $J(H^{2''',5''';3''',6'''}) = 1.6$ Hz, $J(H^{5,6}) = 8.8$ Hz, $J(H^{4,5}) = 5.0$ Hz, $J(H^{4,6}) = 1.6$ Hz. Anal. Calcd for $C_{22}H_{17}F_{12}N_6O_3P_2Re{\cdot}0.5CH_2Cl_2$ ($M_r = 932.0$): C, 29.50; H, 1.95; N, 9.05. Found: C, 29.28; H, 1.95; N, 8.52.

Data for $[(tap)Re(CO)_3(MQ)](PF_6)_2$: δ 4.60 (s, 3H, Me), 7.94 (m, 2H, $H^{3''',5'''}$), 8.46 (d, 2H, $H^{3'',5''}$), 8.63 (s, 2H, $H^{5,6}$), 9.01 (m, 2H, $H^{2''',6'''}$), 9.16 (d, 2H, $H^{2'',6''}$), 9.71 (d, 2H, $H^{2,9}$), 10.04 (d, 2H, $H^{3,8}$); $J(H^{2'',3'';5'',6''}) = 6.8$ Hz, $J(H^{2''',3''';5''',6'''}) = 5.2$ Hz, $J(H^{2''',5''';3''',6'''}) = 1.6$ Hz, $J(H^{2,3;8,9}) = 2.6$ Hz. Anal. Calcd for $C_{24}H_{17}F_{12}N_6O_3P_2Re{\cdot}0.5CH_2Cl_2$ ($M_r = 988.5$): C, 31.55; H, 1.92; N, 8.47. Found: C, 32.74; H, 2.34; N, 8.32.

Data for $[(bpy)Re(CO)_3(mpz)](PF_6)_2$: δ 4.75 (s, 3H, Me), 7.93 (m, 2H, $H^{5,5'}$), 8.49 (t, 2H, $H^{4,4'}$), 8.82 (d, 2H, $H^{3,3'}$), 9.25 (m, 4H, $H^{3'',5''}$ and $H^{6,6'}$), 9.63 (m, 2H, $H^{2'',6''}$); $J(H^{4,5}) = 7.7$ Hz, $J(H^{3,4}) = 8.0$ Hz, $J(H^{3,5}) = 1.2$ Hz. Anal. Calcd for $C_{18}H_{15}F_{12}N_4O_3P_2Re$ ($M_r = 811.2$): C, 26.64; H, 1.86; N, 6.91. Found: C, 26.26; H, 1.93; N, 7.24.

Results and Discussion

Synthesis and Characterization. The compounds $[(N\wedge N)Re(CO)_3(MQ)](PF_6)_2$ ($N\wedge N$ = bpy, bpym) were prepared as reported,[2,9b] and the bpdz and tap analogues and $[(N\wedge N)Re(CO)_3(mpz)](PF_6)_2$ were obtained in a similar manner and characterized by cyclic voltammetry, ^{1}H NMR, IR, and UV/vis absorption spectroscopy. Attempts to obtain complexes with $N\wedge N$ = 2,2′-bipyrazine (bpz) or 4,4′-bipyrimidine (bpm)[9a] failed because of facile complex dissociation. The structures of $[(N\wedge N)Re(CO)_3(MQ)](PF_6)_2$ ($N\wedge N$ = bpy, bpym) confirmed the *fac* configuration of the carbonyl ligands and a twist of about 40° between the pyridyl rings in coordinated MQ^+.[2c,9b] Structural changes with regard to the latter conformation can be expected upon CT excitation[2] or reduction; the reduced MQ system will try to achieve coplanarity because of increasing electron delocalization and bond order between the rings.

Information on the reduced forms of the complexes as obtained through cyclic voltammetry, EPR, IR, and UV/vis spectroelectrochemistry are summarized in Tables 1−4, and

---

(8) Constable, E. C. *Adv. Inorg. Chem.* **1989**, *34*, 1.

(9) (a) Ernst, S.; Kaim, W. *J. Am. Chem. Soc.* **1986**, *108*, 3578. (b) Winslow, L. N.; Rillema, D. P.; Welch, J. H.; Singh, P. *Inorg. Chem.* **1989**, *28*, 1596.

(10) (a) Ernst, S.; Kaim, W. *Inorg. Chim. Acta* **1986**, *114*, 123. (b) Onggo, D.; Rae, A. D.; Goodwin, H. A. *Inorg. Chim. Acta* **1990**, *178*, 151.

(11) (a) Ernst, S.; Vogler, C.; Klein, A.; Kaim, W.; Zalis, S. *Inorg. Chem.* **1996**, *35*, 1295. (b) Vogler, C.; Schwederski, B.; Klein, A.; Kaim, W. *J. Organomet. Chem.* **1992**, *436*, 367.

(12) (a) Jacquet, L.; Davies, R. J. H.; Kirsch-De Mesmaeker, A.; Kelly, J. M. *J. Am. Chem. Soc.* **1997**, *119*, 11763. (b) Kirsch-De Mesmaeker, A.; Nasielski-Hinkens, R.; Maetens, D.; Pauwels, D.; Nasielski, J. *Inorg. Chem.* **1984**, *23*, 377. (c) Jacquet, L.; Kelley, J. M.; Kirsch-De Mesmaeker, A. *J. Chem. Soc., Chem. Commun.* **1995**, 913.

(13) (a) Wishart, J. F.; Bino, A.; Taube, H. *Inorg. Chem.* **1986**, *25*, 3318. (b) Kaim, W.; Kohlmann, S.; Ernst, S.; Olbrich-Deussner, B.; Bessenbacher, C.; Schulz, A. *J. Organomet. Chem.* **1987**, *321*, 215. (c) Bruns, W.; Hausen, H.-D.; Kaim, W.; Schulz, A. *J. Organomet. Chem.* **1993**, *444*, 121. (d) Hilgers, F.; Bruns, W.; Fiedler; J.; Kaim, W. *J. Organomet. Chem.* **1996**, *551*, 273. (e) Matheis, W. Ph.D. Thesis, University of Stuttgart, 1994. (f) Darby, W. L.; Vallarino, L. M. *Inorg. Chim. Acta* **1983**, *75*, 65.

(14) (a) Krejcik, M.; Vlcek, A. A. *J. Electroanal. Chem. Interfacial Electrochem.* **1991**, *313*, 243. (b) Krejcik, M.; Danek, M.; Hartl, F. *J. Electroanal. Chem. Interfacial Electrochem.* **1991**, *317*, 179.

(15) Kaim, W.; Ernst, S.; Kasack, V. *J. Am. Chem. Soc.* **1990**, *112*, 173.

(16) Kaim, W.; Kramer, H. E. A.; Vogler, C.; Rieker, J. *J. Organomet. Chem.* **1989**, *367*, 107.

(17) Klein, A.; Vogler, C.; Kaim, W. *Organometallics* **1996**, *15*, 236.

Table 1. Electrochemical Data[a]

compound	E^{I}	E^{II}	E^{III}	E^{IV}
MQ^+	−1.35 (75)	−2.04 (78)		
$(\mathrm{bpy})\mathrm{Re(CO)_3Cl}^c$	−1.74 (60)	-2.24^b		
$[(\mathrm{bpy})\mathrm{Re(CO)_3(CH_3CN)}]^{+\,d}$	−1.61 (85)	-1.88^b		
$[(\mathrm{bpy})\mathrm{Re(CO)_3(MQ)}]^{2+}$	−1.10 (72)	−1.57 (75)	−1.75 (60)	−2.28 (99)
$(\mathrm{bpym})\mathrm{Re(CO)_3Cl}^c$	−1.42 (80)	-2.04^b		
$[(\mathrm{bpym})\mathrm{Re(CO)_3(CH_3CN)}]^{+\,d}$	−1.38 (70)	-1.74^b		
$[(\mathrm{bpym})\mathrm{Re(CO)_3(MQ)}]^{2+}$	−1.10 (72)	−1.25 (60)	−1.68 (60)	−2.04 (81)
$(\mathrm{bpdz})\mathrm{Re(CO)_3Cl}^c$	−1.39 (70)	-1.91^b		
$[(\mathrm{bpdz})\mathrm{Re(CO)_3(CH_3CN)}]^{+}$	−1.20 (65)	-1.66^b		
$[(\mathrm{bpdz})\mathrm{Re(CO)_3(MQ)}]^{2+}$	−1.10 (58)	−1.17 (70)	−1.63 (80)	−2.04 (82)
$(\mathrm{tap})\mathrm{Re(CO)_3Cl}^c$	−1.18 (65)	-1.73^b		
$[(\mathrm{tap})\mathrm{Re(CO)_3(CH_3CN)}]^{+}$	$-1.12\ (60)^e$			
$[(\mathrm{tap})\mathrm{Re(CO)_3(MQ)}]^{2+}$	−1.05 (50)	−1.35 (55)	−1.64 (70)	−1.86 (82)
mpz^+	-1.15^b			
$[(\mathrm{bpy})\mathrm{Re(CO)_3(mpz)}]^{2+}$	−0.55 (78)	-1.13^b	−1.60 (90)	−1.83 (84)

[a] From cyclic voltammetry in 0.1 M $\mathrm{Bu_4NPF_6/CH_3CN}$ at 100 mV scan rate (single-scan experiments). Potentials for compound reduction in V vs ferrocene/ferrocenium are listed, with peak potential differences in parentheses. [b] Cathodic peak potential for irreversible reduction. [c] In 0.1 M $\mathrm{Bu_4NPF_6}$/DMF (from ref 17). [d] From ref 17.

Figures 1−5 illustrate some of the electrochemical and spectroscopic responses.

Cyclic Voltammetry. All four complexes $[(\mathrm{N}\wedge\mathrm{N})\mathrm{Re(CO)_3(MQ)}](\mathrm{PF_6})_2$ ($\mathrm{N}\wedge\mathrm{N}$ = bpy, bpym, bpdz, tap) undergo four reversible one-electron reduction processes, though at quite different potential values and with different spectroscopic results.

Although the complex ions $[(\mathrm{N}\wedge\mathrm{N})\mathrm{Re(CO)_3(MQ)}]^{2+}$ ($\mathrm{N}\wedge\mathrm{N}$ = bpdz, tap) appear to be stable in acetonitrile solutions, we observed an electron transfer-induced[18] exchange reaction:

$$[(\mathrm{N}\wedge\mathrm{N})\mathrm{Re(CO)_3(MQ)}]^{2+} + \mathrm{CH_3CN} \rightarrow [(\mathrm{N}\wedge\mathrm{N})\mathrm{Re(CO)_3(CH_3CN)}]^{+} + \mathrm{MQ}^{+} \quad (1)$$

In a typical experiment, the working electrode of the OTTLE cell for spectroelectrochemistry was polarized to a potential at the positive base of the voltammetric reduction peak of $[(\mathrm{N}\wedge\mathrm{N})\mathrm{Re(CO)_3(MQ)}]^{2+}$. The complex is then readily converted into the known and spectroscopically characterized species[17] $[(\mathrm{N}\wedge\mathrm{N})\mathrm{Re(CO)_3(CH_3CN)}]^{+}$ without significant formation of reduced forms. Fast reduction of the complexes at more negative potentials (i.e., behind the first reduction peak) produces unsubstituted $[(\mathrm{N}\wedge\mathrm{N})\mathrm{Re(CO)_3(MQ)}]^{\bullet+}$ with only a minor fraction of substituted compound in the case of $\mathrm{N}\wedge\mathrm{N}$ = bpdz.

Following earlier studies[17] we can well conclude that the activation energy for substitution is lower for the reduced states (eq 2) with the $18+\delta$ valence electron configuration at the metal than in eq 1.

$$[(\mathrm{N}\wedge\mathrm{N})\mathrm{Re(CO)_3(MQ)}]^{\bullet+} + \mathrm{CH_3CN} \rightarrow [(\mathrm{N}\wedge\mathrm{N})\mathrm{Re(CO)_3(CH_3CN)}]^{\bullet} + \mathrm{MQ}^{+} \quad (2)$$

Since the half-wave potentials of the acetonitrile complexes $[(\mathrm{N}\wedge\mathrm{N})\mathrm{Re(CO)_3(CH_3CN)}]^{n}$ [17] are slightly more negative (by about 0.1 V) than those of the MQ^+ analogues (Table 1) the oxidation (eq 3) of the transients $[(\mathrm{N}\wedge\mathrm{N})\mathrm{Re(CO)_3(CH_3CN)}]^{\bullet}$ by $[(\mathrm{N}\wedge\mathrm{N})\mathrm{Re(CO)_3(MQ)}]^{2+}$ can close an electrocatalytic[18] cycle.

$$[(\mathrm{N}\wedge\mathrm{N})\mathrm{Re(CO)_3(MQ)}]^{2+} + [(\mathrm{N}\wedge\mathrm{N})\mathrm{Re(CO)_3(CH_3CN)}]^{\bullet} \rightarrow [(\mathrm{N}\wedge\mathrm{N})\mathrm{Re(CO)_3(CH_3CN)}]^{+} + [(\mathrm{N}\wedge\mathrm{N})\mathrm{Re(CO)_3(MQ)}]^{\bullet+} \quad (3)$$

The electron transfer-induced substitution is efficient even when the reduced complex $[(\mathrm{N}\wedge\mathrm{N})\mathrm{Re(CO)_3(MQ)}]^{\bullet+}$ appears thermodynamically stable in acetonitrile solution and hence the species $[(\mathrm{N}\wedge\mathrm{N})\mathrm{Re(CO)_3(CH_3CN)}]^{\bullet}$ can be formed, via eq 2, in only a small “catalytic” amount.

As outlined previously,[11b,17] the difference between the bpy or bpym complexes on one hand and the bpdz or tap systems on the other hand lies in the significantly stronger spin and charge transfer from reduced $\mathrm{N}\wedge\mathrm{N}$ to the metal in the latter cases where large MO coefficients exist at the ligand−metal interface in the lowest-lying π^* orbital.[9a,17] Experimentally, this stronger charge-transfer results in enhanced substitutional lability of axial ligands.[17,19]

Even considering electrocatalytic substitution, the analysis of the reduction of $[(\mathrm{bpdz})\mathrm{Re(CO)_3(MQ)}](\mathrm{PF_6})_2$ solely by cyclic voltammetry (Figure 1) proved to be unsatisfactory, only the use of IR spectroelectrochemistry showed the presence of two close lying but differently located reduction processes (see below).

The variations in electrochemical potential differences (Table 1) do not simply go parallel with the reduction potentials of $\mathrm{N}\wedge\mathrm{N}$: bpy, −2.66 V; bpym, − 2.30 V; bpdz, −2.33 V; tap, −2.00 V.[11b] This already suggests that the electron acquisition sequence may change, depending on the relative acceptor properties of the chelate and the monodentate axial ligand. Spectroelectrochemistry was thus employed to elucidate the location of the first three added electrons for the $[(\mathrm{N}\wedge\mathrm{N})\mathrm{Re(CO)_3(MQ)}]^{n}$ series; the four-electron reduced states $[(\mathrm{N}\wedge\mathrm{N})\mathrm{Re(CO)_3(MQ)}]^{2-}$ were too labile to be studied by that method.

The first reduction of compound $[(\mathrm{bpy})\mathrm{Re(CO)_3(mpz)}](\mathrm{PF_6})_2$ occurs in a cyclovoltammetrically reversible one-electron step at a less negative potential (Table 1) − clear indication for an electron uptake by the mpz^+ ligand.[13] The second reduction wave, at about −1.1 V vs $\mathrm{Fc}^{+/0}$, is not too negative either, but is no longer fully reversible (Figure 2), which may suggest that the second electron also populates the π^*(mpz) orbital, creating

---

(18) (a) Hershberger, J. W.; Klingler, R. J.; Kochi, J. K. *J. Am. Chem. Soc.* **1983**, *105*, 61. (b) Kochi, J. K. *J. Organomet. Chem.* **1986**, *300*, 139. (c) Miholova, D.; Vlcek, A. A. *J. Organomet. Chem.* **1982**, *240*, 413.

(19) Kaim, W.; Olbrich-Deussner, B.; Gross, R.; Ernst, S.; Kohlmann, S.; Bessenbacher, C. In *Importance of Paramagnetic Organometallic Species in Activation, Selectivity and Catalysis*; Chanon, M., Ed.; Kluwer Academic Publishers: Dordrecht, The Netherlands, 1989; p 283.

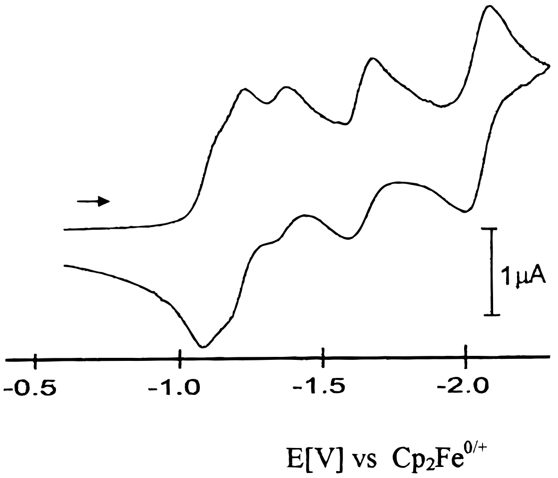

Figure 1. Cyclic voltammogram of $[(bpdz)Re(CO)_3(MQ)](PF_6)_2$ in CH_3CN/0.1 M Bu_4NPF_6 at 100 mV/s scan rate.

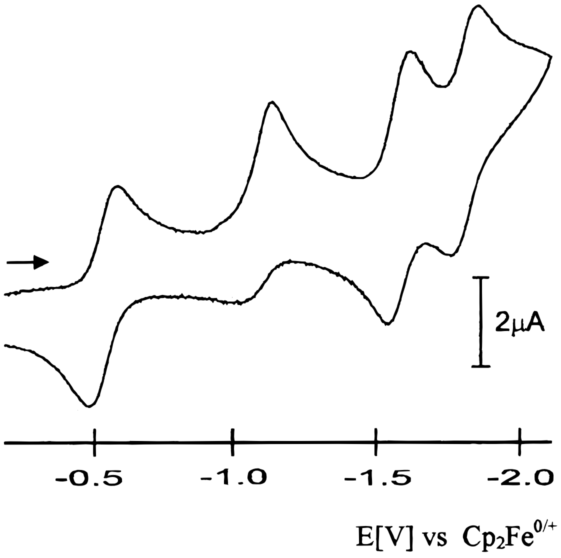

Figure 2. Cyclic voltammogram of $[(bpy)Re(CO)_3(mpz)](PF_6)_2$ in CH_3CN/0.1 M Bu_4NPF_6 at 100 mV/s scan rate.

an unstable 8 π electron species.[7,20] The two following reversible waves at more negative potential values are those of the substitution product $[(bpy)Re(CO)_3(CH_3CN)]^n$ (Table 1).[17] Unfortunately, even the first reduction process is not sufficiently reversible for OTTLE spectroelectrochemistry which requires stability of the generated intermediates of a few minutes; observation of $mpzH^{\bullet+}$ [21] by the EPR confirms this lability (see below).

Electron Paramagnetic Resonance. The EPR results for the one-electron reduction products $[(N{\wedge}N)Re(CO)_3(MQ)]^{\bullet+}$ of the MQ complexes are not unequivocal with respect to the spin location. Due to the typically broad lines in such rhenium(I) radical complexes[17,22] the only extractable hyperfine coupling for $[(bpy)Re(CO)_3(MQ)]^{\bullet+}$ ($g = 2.0028$) is that of $^{185,187}Re$ ($I = {}^5/_2$) which gives rise to the familiar[17,22] "two-line pattern" of Figure 3. At 0.92 mT the metal hyperfine coupling is slightly smaller than the 1.2 mT for $[(bpy)Re(CO)_3Cl]^{\bullet-}$ ($g = 2.0032$);[17,22] similarly small metal hyperfine splittings were determined for $[(bpym)Re(CO)_3(MQ)]^{\bullet+}$ and $[(bpdz)Re(CO)_3(MQ)]^{\bullet+}$ (Table 2). These small effects on a($^{185,187}Re$) and g values do not allow us to make a definite distinction between a coordinated $MQ^{\bullet}$ radical or a bound α-diimine anion radical ligand. Rhenium hyperfine coupling between 1.0 and 3.8 mT has been observed for the latter situation $(N{\wedge}N^{-I})Re(CO)_3(X)$,[17,22] whereas rhenium(I) complexes with axially bound radical ligands as used here have not yet been reported.[23]

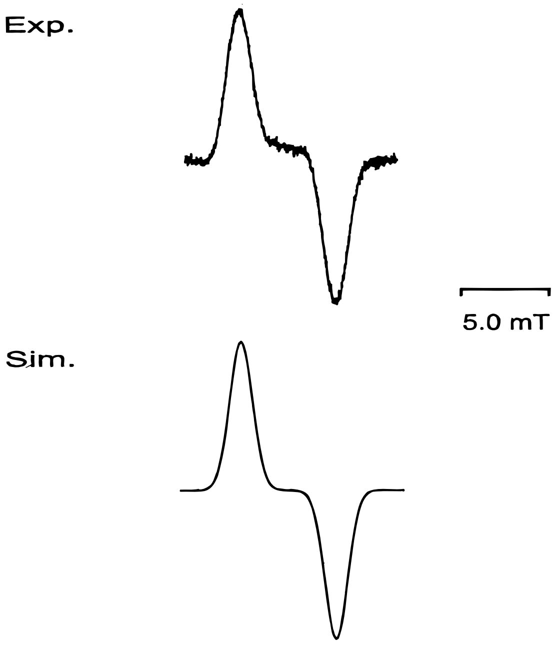

Figure 3. EPR spectrum of of $[(bpy)Re(CO)_3(MQ)]^{\bullet+}$ generated by reduction in CH_3CN/0.1 M Bu_4NPF_6 (top); computer-simulated spectrum with a ($^{185,187}Re$) = 0.92 mT and a 1.4 mT Gaussian line width (bottom).

Table 2. EPR Data of Paramagnetic Complexes[a]

radical complex	a_{Re}[b]	g
$[(bpy)Re(CO)_3Cl]^{\bullet-}$	1.20	2.0032
$[(bpy)Re(CO)_3(MQ)]^{\bullet+}$	0.92	2.0028
$[(bpym)Re(CO)_3Cl]^{\bullet-}$	1.00	2.0026
$[(bpym)Re(CO)_3(MQ)]^{\bullet+}$	0.90	2.0036
$[(bpdz)Re(CO)_3Cl]^{\bullet-}$	1.4	2.0018
$[(bpdz)Re(CO)_3(CH_3CN)]^{\bullet}$	1.82	nd
$[(bpdz)Re(CO)_3(MQ)]^{\bullet+}$	1.12	2.0020
$[(tap)Re(CO)_3Cl]^{\bullet-}$	1.6	2.0003
$[(tap)Re(CO)_3(MQ)]^{\bullet+}$ [c]		$g_1 = 2.0470$ $g_2 = 2.0033$ $g_3 = 1.9670$
$[(bpy)Re(CO)_3(mpz)]^{\bullet+}$	1.98[d]	2.0044

[a] From measurements in 0.1 M Bu_4NPF_6/CH_3CN at 250 K. [b] $^{185,187}Re$ coupling constant (in mT) from computer simulated spectra. ^{185}Re, 37.4% natural abundance, $I = {}^5/_2$; ^{187}Re, 62.6%, $I = {}^5/_2$, 1% difference in nuclear magnetic moments. [c] Signal not observed at 250 K; g factor components determined at 110 K in glassy frozen solution. [d] Additional coupling of about 0.8 mT.

Despite this ambiguity, the very different electronic structure of the tap analogue is apparent from the unusual EPR behavior of $[(tap)Re(CO)_3(MQ)]^{\bullet+}$. It does not exhibit an EPR signal at room temperature, presumably due to rapid relaxation; broad rhombic features with $g_1 = 2.0470$, $g_2 = 2.0033$, and $g_3 = 1.9670$ appear at low temperatures (110 K) in frozen acetonitrile solution. While the apparent rapid relaxation suggests the presence of excited states lying close to the doublet ground

---

(20) Kaim, W. *Rev. Chem. Intermed.* **1987**, *8*, 247.

(21) Kaim, W. *J. Chem. Soc., Perkin Trans. 2* **1984**, 1357.

(22) (a) Kaim, W.; Kohlmann, S. *Chem. Phys. Lett.* **1987**, *139*, 365. (b) Kaim, W.; Kohlmann, S. *Inorg. Chem.* **1990**, *29*, 2909.

(23) For EPR features of metal-based spin on rhenium, see, for instance: Banerjee, S.; Dirghangi, B. K.; Menon, M.; Pramanik, A.; Chakravorty, A. *J. Chem. Soc., Dalton Trans.* **1997**, 2149.

state,[24] the g anisotropy $\Delta g = g_1 - g_3 = 0.080$ and the average $\langle g \rangle = 2.0058$ are still in agreement with ligand based spin.[22−24] The close-lying states could involve either one of the energetically similar $b_1(\psi)$ or $a_2(\chi)$ π^* orbitals of tap[11] and/or the π^* MO of MQ^+.

In situ EPR spectroscopy after reduction of $[(bpy)Re(CO)_3(mpz)](PF_6)_2$ in acetonitrile/0.1 M Bu_4NPF_6 reveals the generation both of $[(bpy)Re(CO)_3(mpz)]^{\bullet+}$ with $g = 2.0044$, $a(^{185,187}Re) = 1.98$ mT and some partially resolved ligand hyperfine coupling of about 0.8 mT, and of $mpzH^{\bullet+}$ [21] with $g = 2.0034$ (from dissociation and proton addition). In the case of $[(bpy)Re(CO)_3(MQ)]^n$ the signal of the corresponding metal-free radical $MQH^{\bullet+}$ appears only after prolonged electrolysis (>15 min). The higher metal coupling constant in $[(bpy)Re(CO)_3(mpz)]^{\bullet+}$ supports the location of spin on the axial monoquaternized ligand; $mpz^\bullet$ has a much higher spin population on the metal-coordinating nitrogen center than the larger π system $MQ^\bullet$.[13c−f]

UV/Vis Spectroelectrochemistry. One-electron reduced 4,4′-bipyridinium systems and α-diimine anion radicals contain related chromophors but exhibit different absorption spectra in the long-wavelength region.[5,6,25] The former have mainly intense bands around 600 nm which convey a deep bluish color (hence the term “viologens” for the precursors).[6,26] Absorptions at longer wavelengths are usually very weak due to the symmetry of the 4,4′-bipyridinium chromophore. The lower symmetric $(\alpha\text{-diimine})^{\bullet-}$ species, on the other hand, generally display well-detectable bands in the near-infrared region (>750 nm) with distinct vibrational fine structuring.[5] In the two-electron reduced forms both kinds of π systems display intense features around 400 nm.

In the present case, the complex ion $[(bpy)Re(CO)_3(MQ)]^{2+}$ shows the emergence of an intense 599 nm band after the first one-electron uptake (Figure 4), in agreement with the formulation of a MQ^+-centered reduction in Scheme 1. On further reduction, this feature is somewhat diminished, an additional intense band system emerges at about 400 nm, and a weak, broad band appears in the 800−900 nm region (Figure 4). This observation is compatible with a situation where the bpy ligand has taken up the second electron: $\lambda_{max}(bpy^{\bullet-})$: 882, 582, 397 nm (maxima of band systems in DMF).[5a] Addition of yet another electron causes the 599 nm band system to disappear while the features at ∼400 and ∼850 nm remain (Figure 4, Table 3). Both observations suggest a reduction of $MQ^\bullet$ to MQ^- while the chelate ligand remains as coordinated anion radical.

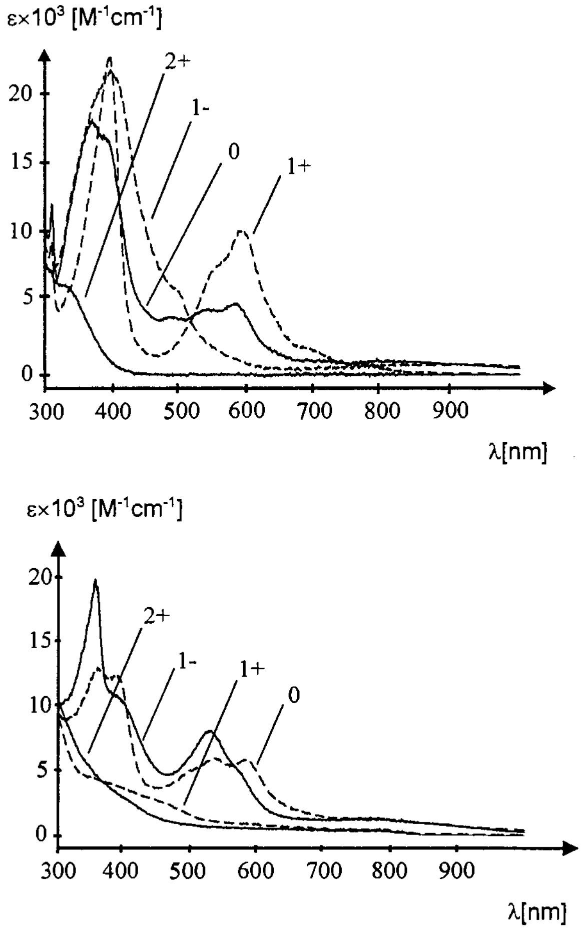

Figure 4. Absorption spectra of $[(bpy)Re(CO)_3(MQ)]^n$ (top) and $[(tap)Re(CO)_3(MQ)]^n$ (bottom) from OTTLE cell spectroelectrochemistry in CH_3CN/0.1 M Bu_4NPF_6.

Scheme 1

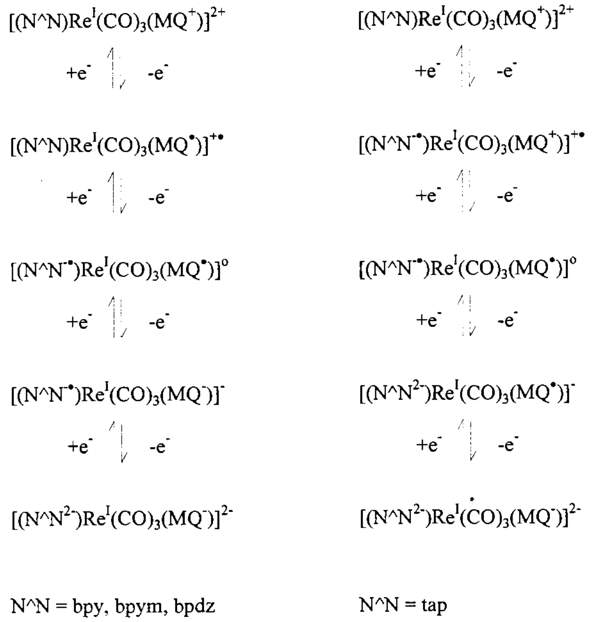

The analogous complexes, bpym and bpdz ligand π systems[5c] display a similar behavior as the bpy compound (Table 3). However, reduction of $[(tap)Re(CO)_3(MQ)]^{2+}$ yields quite a different pattern of spectra (Figure 4). One-electron reduction to the cation radical produces only marginal changes in the visible and near-UV parts of the spectrum; in particular, there is no strong absorption emerging at about 600 nm as would be required for the formation of the MQ radical. We thus conclude that the first reduction takes place at the chelate ligand and not, as in the bpy system, on the MQ^+ axial ligand (Scheme 1). Only the second added electron produces an intense absorption band system in the 500−600 nm region (Figure 4), indicating the formation of $MQ^\bullet$. This band remains in slightly differently structured form after uptake of the third electron, suggesting that the α-diimine picks up this third electron to form a two-electron reduced ligand before the axial ligand does likewise (Scheme 1).

IR Vibrational Spectroelectrochemistry. Reduction of carbonylmetal complexes generally results in a decrease of the

---

(24) (a) Kaim, W. *Coord. Chem. Rev.* **1987**, *76*, 187. (b) Poppe, J.; Moscherosch, M.; Kaim, W. *Inorg. Chem.* **1993**, *32*, 2640.

(25) Shida, T. *Electronic Absorption Spectra of Radical Ions*; Elsevier: Amsterdam, 1988.

(26) Zalis, S.; Krejcik, M.; Drchal, V.; Vlcek, A. A. *Inorg. Chem.* **1995**, *34*, 6008.

Table 3. Absorption Maxima[a] from UV/NIR Spectroelectrochemistry[b]

	n			
compound	2+	1+	0	1−
MQ^n		259	249 286 370 536	
$[(bpy)Re(CO)_3(MQ)]^n$	251 (19.9) 312 (9.7) 320 (11.7) 341 (5.9)	249 (12.3) 305 sh (9.3) 320 (9.1) 408 (22.2) 563 sh (7.3) 599 (9.8) 703 sh, br (1.6)	250 sh (11.4) 292 (10.0) 382 (17.7) 404 sh (16.4) 500 sh (3.8) 552 sh (4.3) 592 (4.7) 840 br (0.6)	265 sh (12.5) 410 (21.2) 507 sh (5.8)
$[(bpym)Re(CO)_3(MQ)]^n$	250 (23.2) 318 sh (6.6)	246 (16.5) 305 sh (5.5) 407 (15.9) 562 sh (4.9) 597 (6.3) 704 sh, br (1.3)	296 sh (9.1) 342 sh (10.5) 372 (14.9) 405 sh (12.5) 488 (4.5) 551 (5.5) 594 (5.5) 853 br (1.1)	340 sh (10.6) 380 sh (17.0) 410 (19.9) 495 sh (5.5) 541 sh (2.0)
$[(bpdz)Re(CO)_3(MQ)]^n$	255 (22.1) 330 (5.3) 390 (3.1)	259[c] 315 sh 405 555 sh 593 799 br	259 sh (14.8) 373 (17.9) 403 (19.1) 549 (8.8) 591 (9.2) 800 br (1.2)	252 sh (18.6) 371 (20.5) 528 (10.9) 615 sh (3.7)
$[(tap)Re(CO)_3(MQ)]^n$	254 (17.8) 292 (16.2)	259 (18.9) 303 (11.2) 400 sh, br (4.2)	254 (13.0) 301 (11.7) 374 (13.7) 403 sh (13.2) 505 sh (5.1) 549 (6.3) 596 (6.2) 785 (2.3)	250 (14.0) 301 (10.6) 370 (21.1) 407 sh (11.3) 539 (8.6) 785 (1.3)

[a] Absorption maxima λ_{max} in nm, molar absorption coefficients $\epsilon \times 10^{-3}$ (in parentheses) in $M^{-1}\,cm^{-1}$. [b] From measurements in 0.1 M Bu_4NPF_6/CH_3CN. [c] $[(bpdz)Re(CO)_3(MQ)]^{\bullet+}$ could be generated only to about 70% within the disproportionation equilibium (4).

CO stretching frequencies.[3] This effect, indicating increased back-donation from a more electron-rich metal center, occurs even when the electron is not added to the metal itself but to a coordinated ligand.[4] While the absolute shifts $\Delta\nu$(CO) cannot be directly taken as a measure of transferred charge,[4] the comparison between the compounds discussed here is still quite revealing. The observed shifts (Figure 5, Table 4) for the A_1 and E bands (spectroscopic C_{3v} symmetry[17]) exhibit a dichotomous pattern: for N∧N = bpy, bpym and bpdz, the shift sequence is small/large/small for the first three reduction processes whereas the opposite is true for the complex $[(tap)Re(CO)_3(MQ)]^n$. Assuming the sequence from Scheme 1 (which is already supported by cyclic voltammetry, EPR, and UV/vis spectroelectrochemistry), we conclude that electron addition to the N∧N chelate ligand produces a greater shift $\Delta\nu$(CO) than electron uptake by MQ^+. This result confirms the stronger ligand-to-metal spin transfer from the bidentate ligand as is evident also from EPR spectroscopy where tricarbonylrhenium(I) complexes of α-diimine anion radicals exhibit large ^{185,187}Re hyperfine values betwen 1.2 and 3.8 mT[17] whereas $[(N{\wedge}N)Re(CO)_3(MQ)]^{\bullet+}$ yield only a(^{185,187}Re) = 0.9−1.2 mT (Table 2).

Analysis of the bpdz Complex. The cyclovoltammetric response of $[(bpdz)Re(CO)_3(MQ)]^{2+}$ in acetonitrile solution (Figure 1) is complicated due to electrocatalyzed exchange processes 1−3 described above. Substitution of the ligand MQ^+ is induced when the electrode potential is established at the base of the first cathodic voltammetric peak. The resulting carbonyl vibrational spectrum corresponds to the spectrum of an authentic sample of $[(bpdz)Re(CO)(CH_3CN)](PF_6)$.[17] On the other hand, when the electrode potential is scanned up to a potential behind that first voltammetric peak, the IR bands corresponding to the unsubstituted reduced forms appear and only minor amounts of the substituted species $[(bpdz)Re(CO)_3(CH_3CN)]^\bullet$ are detected in the resulting solution. The concentration profiles of nonreduced, one-electron reduced, and two-electron reduced forms of the MQ-containing complex as derived from the carbonyl vibrational bands (Table 4) during the reduction are shown in Figure 6. The one-electron reduction product is formed in only about 70% yield when 1 equiv (1 F/mol) is passed through; the other two forms of the disproportionation equilibrium exist simultaneously in solution.

$$\underset{\mathbf{1}}{2[(bpdz)Re(CO)_3(MQ)]^{\bullet+}} \rightleftharpoons \underset{\mathbf{0}}{[(bpdz)Re(CO)_3(MQ)]^{2+}} + \underset{\mathbf{2}}{[(bpdz)Re(CO)_3(MQ)]} \quad (4)$$

The corresponding curves in Figure 6 are constructed on the basis of equations describing the system

$$K = \frac{[\mathbf{0}][\mathbf{2}]}{[\mathbf{1}]^2}$$

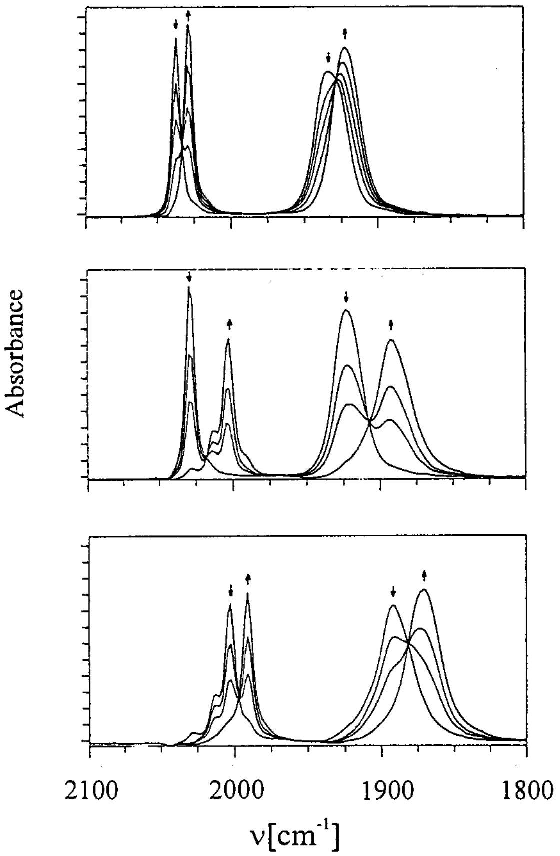

Figure 5. Carbonyl vibrational spectra of $[(bpy)Re(CO)_3(MQ)]^n$ (n = 2+ → 1+ (top); n = 1+ → 0 (middle); n = 0 → 1− (bottom)) from OTTLE cell spectroelectrochemistry in CH_3CN/0.1 M Bu_4NPF_6.

Table 4. Data from IR Spectroelectrochemistry[a]

compound	ν_{CO} (cm^{-1})	
$[(bpy)Re(CO)_3(MQ)]^n$		
$n = 2+$	2037	1934
$n = 1+$	2029	1923
$n = 0$	2003	1892
$n = 1-$	1991	1870
$[(bpym)Re(CO)_3(MQ)]^n$		
$n = 2+$	2042	1944
$n = 1+$	2033	1931
$n = 0$	2012	1900
$n = 1-$	1998	1881
$[(bpdz)Re(CO)_3(MQ)]^n$		
$n = 2+$	2044	1934
$n = 1+^b$	2030	1908
$n = 0$	2005	1893
$n = 1-$	1992	1860
$[(tap)Re(CO)_3(MQ)]^n$		
$n = 2+$	2048	1950
$n = 1+$	2019	1918
$n = 0$	2014	1906
$n = 1-$	1998	1871
$[(bpy)Re(CO)_3(mpz)]^n$		
$n = 2+$	2044	1948

[a] From OTTLE measurements in 0.1 M Bu_4NPF_6/CH_3CN. [b] $[(bpdz)Re(CO)_3(MQ)]^{\bullet +}$ could be generated only to about 70% within the disproportionation equilibrium (4).

where [**0**] + [**1**] + [**2**] = 1, n = [**1**] + 2[**2**], and K is a disproportionation constant.

[**0**], [**1**], and [**2**] denote relative concentrations of nonreduced, one-electron reduced, and two-electron reduced forms, respectively, and n is the number of electrons (F/mol) passed. Arithmetic rearrangement leads to explicit expressions for the concentrations as a function of the charge passed:

$$[\mathbf{1}] = \frac{\sqrt{1 - (4K - 1)(n^2 - 2n) - 1}}{4K - 1}$$

$$[\mathbf{2}] = \frac{n - [\mathbf{1}]}{2}$$

$$[\mathbf{0}] = 1 - [\mathbf{1}] - [\mathbf{2}]$$

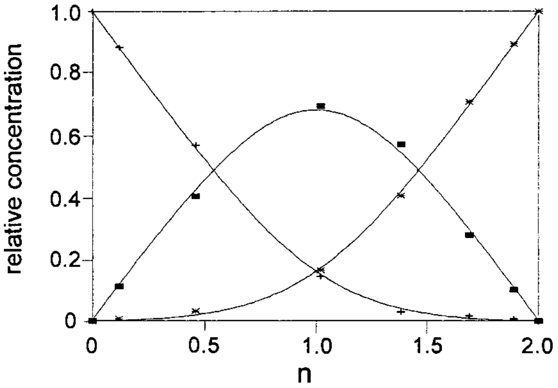

Figure 6. Concentration profiles during reduction of $[(bpdz)Re(CO)_3(MQ)](PF_6)_2$ based on IR spectroelectrochemistry in CH_3CN/0.1 M Bu_4NPF_6 (n, number of electron equivalents; +, dication; ■, monocation; *, neutral species).

The experimental data are reasonably reproduced by the curves calculated for $K = 0.055$ (Figure 6).

The disproportionation constant is related to the difference of half-wave potentials for the second and first electron transfer by $RT \ln K = nF\Delta E_{1/2}$, the value $K = 0.055$ corresponding to $\Delta E = -74$ mV. Hence, the experimentally observed cyclovoltammetric response can be interpreted as a convoluted signal which contains the first and second one-electron reduction steps ($E_{1/2}{}^{I} = -1.10$ V; $E_{1/2}{}^{II} = -1.17$ V) and adjacent peaks due to $[(bpdz)Re(CO)_3(CH_3CN)]^+$ ($E_{1/2} = -1.20$ V) and free MQ^+ ($E_{1/2} = -1.35$ V) formed from electron-transfer catalyzed ligand exchange at the electrode. Two further reduction processes are observed at more negative potentials (Table 1) as well separated voltammetric peaks.

Conclusion

We have shown that UV/vis absorption and especially IR spectroelectrochemistry are well suited to elucidate the nature of the individual redox states in complexes with several redox-active functions such as $[(N{\wedge}N)Re(CO)_3(L)]^n$. While not being sufficiently indicative alone, cyclic voltammetry and EPR are also in agreement with the sequence summarized in Scheme 1 and illustrated in Figure 7.

Using the different α-diimine ligands N∧N = bpy, bpym, bpdz, or tap in complexes $[(N{\wedge}N)Re(CO)_3(MQ)]^n$ we were thus able to prove a reversal in electron uptake sequences between the two kinds of heterocyclic ligands. Obviously, the π^* MO of electron-accepting tap[11] lies below the π^* orbital of coordinated MQ^+, while the reverse holds for the complexes with bpy, bpym, and bpdz. On the basis of the spectroelectrochemical results we can thus assign the electrochemical processes in $[(N{\wedge}N)Re(CO)_3(MQ)]^n$, revealing little-changed potentials for the $MQ^{+/\bullet}$ and $MQ^{\bullet/-}$ pairs and anodic shifts of the N∧N-based potentials. The complex with N∧N = bpdz in particular lies very close to the switch point between both situations, the analysis using carbonyl vibrational spectroelectrochemistry

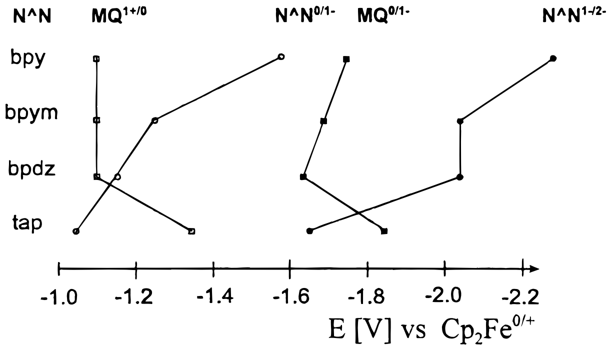

Figure 7. Assignment of ligand reduction processes for complexes $[(N\wedge N)Re(CO)_3(MQ)]^n$, based on cyclovoltammetry and spectroelectrochemistry in CH_3CN/0.1 M Bu_4NPF_6.

yielded a difference of only 74 mV between the potentials. Despite this small difference there appears to be no detectable interaction between the orthogonal π systems of bpdz and MQ^+. The potential for such interaction is higher in complexes $[M(N\wedge N)_3]^k$ with 60° dihedral angles between ligand π planes.[26] Replacing MQ^+ with the better π accepting but weaker basic (and thus weaker bonded) mpz^+ monodentate ligand clearly revealed the occupation of the $\pi^*(mpz^+)$ orbital on reduction of $[(bpy)Re(CO)_3(mpz)]^{2+}$. For further work, we intend to study the magnetic resonance behavior of carefully generated doubly and triply reduced forms, the former being possible candidates for triplet species with two rather different radical ligands. The demonstrated possibility to tune the sequence of accessible reduced states may well be extended to excited-state tuning and the control of intramolecular electron transfer.[2]

Acknowledgment. This work was supported by Deutsche Forschungsgemeinschaft, Volkswagenstiftung, and Fonds der Chemischen Industrie.

IC980268F